Closed-loop recyclability of a biomass-derived epoxy-amine thermoset by methanolysis

Xianyuan Wu, Peter Hartmann, Dimitri Berne, Mario de Bruyn, Florian Cuminet, Zhiwen Wang, Johannes Matthias Zechner, Adrian Daniel Boese, Vincent Placet, Sylvain Caillol, et al.

Title: Closed-loop recyclability of a biomass-derived epoxy-amine thermoset by methanolysis

Authors: Xianyuan Wu[1,2], Peter Hartmann[2], Dimitri Berne[3], Mario De bruyn[2], Florian Cuminet[3], Zhiwen Wang[2], Johannes Matthias Zechner[2], Adrian Daniel Boese[2], Vincent Placet[4], Sylvain Caillol[3], and Katalin Barta[2]*

Affiliations:

[1]Stratingh Institute for Chemistry, University of Groningen, Groningen, Nijenborgh 4, 9747AG, Groningen, The Netherlands.

[2] Institute of Chemistry, Organic and Bioorganic Chemistry, University of Graz, Heinrichstrasse 28/II, 8010 Graz, Austria

[3]ICGM, Univ Montpellier, CNRS, ENSCM, Montpellier, France

[4]Université Franche-Compte instead of Université Franche-Comté

*Corresponding author. Email: katalin.barta@uni-graz.at

Abstract:

Epoxy resin thermosets (ERTs) are an important class of polymeric materials. However, owing to their highly cross-linked nature, they suffer from poor recyclability, which contributes to an unacceptable level of environmental pollution. There is a clear need for the design of inherently recyclable ERTs based on renewable resources. Here we present the synthesis and closed-loop recycling of a fully lignocellulose-derivable epoxy resin (DGF/MBCA), prepared from dimethyl ester of 2,5-furandicarboxylic acid (DMFD), 4,4'-methylenebis(cyclohexylamine) (MBCA) and glycidol, which displays excellent thermo-mechanical properties (T_g= 170 °C, $E'_{25°C}$ = 1.2 GPa). Surprisingly, the material undergoes methanolysis in the absence of any catalyst, regenerating 90% of the original DMFD. Subsequently the diamine MBCA and glycerol can be reformed by acetolysis. Application and recycling of DGF/MBCA in glass and wood fiber composites are demonstrated.

One-Sentence Summary: High-performance bio-derived epoxy-amine thermoset with inherent recyclability and a proven application range.

Main Text:

Epoxy resin thermosets (ERTs) are an important class of polymeric materials, characterized by high durability and excellent thermal stability, indispensable in many industrial applications such as packaging, construction, transportation, and aviation (*1-3*). However, the general non-recyclability of cured ERTs, a matter that relates to their highly cross-linked nature, poses unacceptable environmental challenges (*4-5*). Moreover, ERTs are typically manufactured from fossil-derived Bisphenol-A (BPA), which has been identified as an endocrine disruptor (*6-7*); Therefore, it is vitally important to find suitable replacements, preferably derived from renewable resources (*8-11*).

Overall, the development of sustainable and circular strategies, and especially closed-loop recycling approaches, for ERTs requires a mindful structural and molecular design. Such innovative design should apply biomass-derivable building blocks, confer excellent thermal-mechanical performance, and impart inherent ERT recyclability (*12*).

The incorporation of dynamic covalent linkages into the polymer backbone represents a major scientific advance in the development of chemically degradable and/or reusable polymers, including ERTs, albeit typically demonstrated for fossil-based building blocks (*13-17*). More recently, cleavable/dynamic linkages such as imines, acetals, and esters have been incorporated into ERT, using renewable building blocks including vanillin (*18-19*), ferulic acid (*20*), 2,5-furan dicarboxylic acid (*21*), naringenin (*22*) or soybean oils (*23*), yet only a few of these materials were fully biomass-based (*8*). Although these excellent studies have achieved degradation/solubilization of the typically insoluble ERT materials, or demonstrated use/reuse loops in vitrimers, the full recovery of the original monomers remains difficult to realize. Nonetheless, beyond (partial) degradation, the development of closed-loop recycling methodologies is of particular importance to enable a truly circular strategy in the use of ERTs (*24*). Closed-loop strategies for fossil-based thermosets have been addressed in pioneering materials science studies by focusing on structural re-design (*25*) or enabling recycling of existing thermoset materials (*26*), while the field of catalysis has focused on the challenging catalytic deconstruction of typical (e.g. bisphenol-A-based) materials by cleavage and activation of the recalcitrant C-N/C-O bonds (*27-30*). Despite these important advances, true closed-loop recycling strategies for entirely bio-based ERTs have not yet been demonstrated.

Here we show that the judicious combination of building blocks derived entirely from lignocellulosic biomass leads to the synthesis of ERTs with excellent thermal and mechanical performance and inherent recyclability. Specifically, the ERT prepared from dimethyl ester of 2,5-furandicarboxylic acid (DMFD), 4,4'-methylenebis(cyclohexylamine) (MBCA) and glycidol (DGF/MBCA) displays excellent thermal-mechanical properties (T_g= 170 °C, $E'_{25°C}$ = 1.2 GPa), even outperforming its reference counterpart made from BPA. Due to its unique chemical structure and morphology, the material can promote its own low temperature depolymerization in methanol, in the absence of any added catalyst. This process leads to full solubilization of the material and excellent recovery of the original furan building block DMFD. Subsequently, given complete material solubilization, we have developed an acetolysis method that regenerates the diamine MBCA and glycerol, thereby closing the recycling loop. Moreover, this inherently recyclable and performance-advantaged DGF/MBCA ERT enables the preparation of reusable glass-fiber and plant-fiber composites.

The developed low temperature methanolysis methodology was adaptable to a small library of additional ERTs, enabling the potential customization of these materials for different application areas.

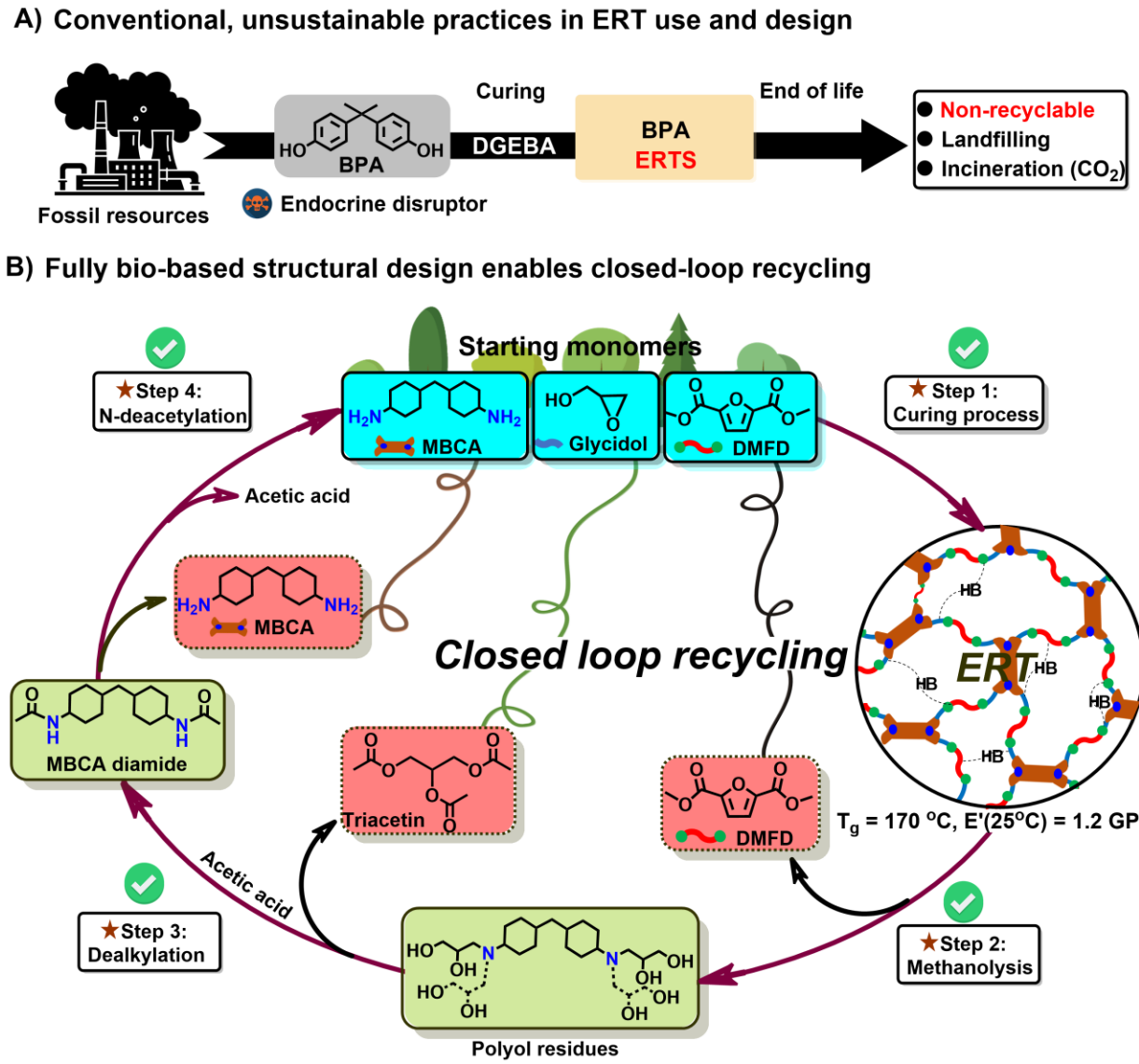

Figure 1. Schematic representation of conventional practices compared to this work with regards to ERT synthesis and recycling. A) The unsustainable status quo of BPA-based thermosets sourced from fossil resources. **B)** Synthesis and closed-loop recyclability of a fully biomass-derivable ERT. **Step 1:** The synthesis of a fully bio-based ERT which can be sustainably sourced from lignocellulose-derived platform chemicals (namely MBCA, glycidol and DMFD) and displays competitive or even enhanced properties to reference BPA-based ERT; **Step 2:** Low-temperature methanolysis of the bio-based DGF/MBCA without any catalyst added; **Step 3:** Acetolysis of the polyol residues fraction, yielding MBCA diamide and triacetin; **Step 4:** N-deacetylation of the MBCA diamide to its initial monomer MBCA demonstrating closed-loop recyclability. HB: hydrogen bond.

Thermoset development and characterization

Targeting improved ERT recyclability, we chose to move away from the typical bisphenol-based diglycidyl-ether structures and aimed to explore ERT derived from diglycidyl esters of 2,5-furane dicarboxylic acid (FDCA) and terephthalic acid (TPA), inspired by pioneering work in this area (*21*,*31-37*) (**Figure 2**). Due to its significance in manufacturing renewable polyesters, FDCA has already gained ample industrial interest (*38-39*). The corresponding, entirely biomass-derivable diglycidyl ester of 2,5-furandicarboxylic acid (DGF) can be smoothly obtained by direct transesterification of dimethyl 2,5-furan dicarboxylate (DMFD) and glycidol (*40*).

Recently we have reported on an efficient catalytic procedure to turn industrially relevant lignin side-streams originating from the paper and pulp industry into well-defined 4,4'-methylenebis(cyclohexylamine) (MBCA) in high overall yields and demonstrated the utility of this unique aliphatic diamine in the development of high performance polybenzoxazine thermosets (*41*). Encouraged by this result, we set out for the evaluation of MBCA as curing agent in the development of ERT, aiming for favorable thermo-mechanical properties.

Indeed, applying MBCA as curing agent together with DGF in a 2:1 ratio, led to the development of the polymer DGF/MBCA, that displays both a markedly high T_g (170 °C) and storage modulus ($E'_{25°C}$ = 1.2 GPa) (**Figure 2, entry 1**).

Following the same synthesis procedure, three other reference thermosets were prepared by variation of either the diamine or the diglycidyl ester monomer. DGF/DDM was obtained by using the aromatic 4,4'-diaminodiphenylmethane (DDM) as curing agent instead of MBCA (**Figure 2, entry 2**). Furthermore, DGB/MBCA and DGEBA/MBCA were obtained by applying MBCA as curing agent and diglycidyl ester of terephthalic acid (DGB) or the diglycidyl-ether of BPA (DGEBA), respectively (**Figure 2, entries 3 and 4**). The successful synthesis of the above-mentioned ERTs was confirmed using both FT-IR (**Figure S15)** and solid-state ^{13}C NMR spectroscopy (**Figure S17**).

Substituting MBCA by the aromatic DDM decreased the T_g value to 162 °C and the storage modulus at 25 °C ($E'_{25\,°C}$) to 0.98 GPa. (**Figure 2, entry 2**), clearly underlining the beneficial effect of the aliphatic MBCA diamine unit. The BPA containing thermoset, DGEBA/MBCA displayed an equally high T_g value as recorded for DGF/MBCA but reached only half its storage modulus (**Figure 2, entry 4**). All thermosets displayed excellent thermal stability ($T_{5\%}$ > 275 °C), with the best value obtained for DGEBA/MBCA ($T_{5\%}$ = 368 °C). The lower $T_{5\%}$ values for DGF/MBCA, DGF/DDM and DGB/MBCA are likely related to the presence of ester functionalities in the polymer strands (*31-33*).

The prepared ERTs were benchmarked against commercial fossil-derived BPA-based thermosets as well as several biomass-derivable ERT materials described in recent literature (**Figure 2**, **entries 5, 6** and **7**; For detailed benchmarking comparison see also **Supplementary Materials section 3.17**), with promising outcome. Our DGF/MBCA ERT displayed a distinct advantage on T_g value compared to various other biomass-based ERT, opening possibilities for potential applications in engineering fields, where a high T_g value (>150 °C) is typically required, while the E' value was perfectly comparable to other bio-based ERTs. Gratifyingly, our DGF/MBCA also showed competitive properties to commercial, fossil-based ERTs (EPON resin 828), cured by DDM or DDS, namely DGEBA/DDM (T_g = 152 °C/$E'_{25\,°C}$ = 2.25 GPa) and DGEBA/DDS (T_g = 200 °C/$E'_{25°C}$ = 1.3 GPa), respectively, indicating that similar industrial applications can be envisioned in the field of adhesives, casting, moldings, electrical laminates, structural laminates, and filament winding (*42*).

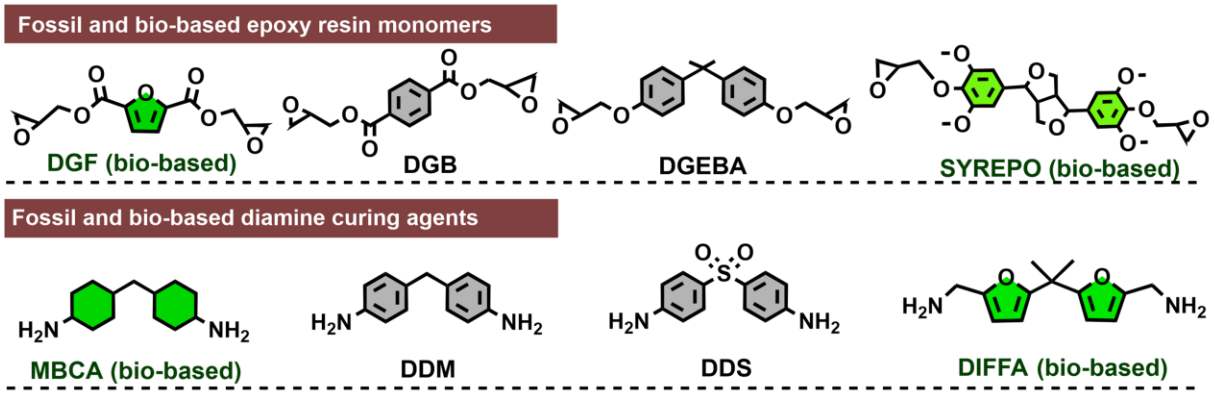

The thermal and mechanical properties of the synthesized epoxy resin[*]

Entry	Epoxy monomer	Diamine	$T_{d5\%}$ (°C)	T_g (°C)	E' (GPa)	GC[¶] (%)	Ref.
1	DGF[§]	MBCA	280	170	1.19	99	This work
2	DGF	DDM	278	162	0.98	98	This work
3	DGB[†]	MBCA	304	169	-	99	This work
4	DGEBA	MBCA	368	168	0.63	100	This work
Benchmarking comparisons of industrially related fully bio-based ERTs							
5	DGEBA[‡]	DDM	359	152	2.25	N.D.	*43*
6	DGEBA[‡]	DDS	343	200	1.3	N.D.	*44*
7	SYREPO[§]	DIFFA	288	102	1.1	N.D.	*45*

[*]. Diamine (1 equiv.) and epoxy monomer (2 equiv.) were cured at 80 °C for 2 h, 150 °C for 8 h, and 170 °C for 1 h; [†]. Difficulty in obtaining reliable storage modulus (E') during the preparation of DGB/MBCA ERT, due to the preparation protocol, which involves a solvent; [‡]. Industrially related DGEBA epoxy resins; [§]. Fully bio-based epoxy resin; [¶]. GC (gel content) was obtained based on the equation referred to supplementary information;

Figure 2. Synthesis and characterization of novel DGF/MBCA ERT and analogues and benchmarking comparisons with industrially relevant DGEBA ERTs as well as recently developed biomass-based ERTs.

The unique low-temperature depolymerization behavior of DGF/MBCA by methanolysis

With DGF/MBCA, DGF/DDM, DGB/MBCA bearing distinct ester functionalities in their polymeric backbones, we set out to investigate the recycling of these ERTs by methanolysis (**Figure 3**) (*46-47*). Remarkably, the fully cured DGF/MBCA (see **Figure S15, S18**) readily dissolved in methanol in the absence of any additives at 70 °C, and the simultaneously observed white precipitate was found to be highly pure DMFD, one of the original monomers (^{1}H and ^{13}C NMR analysis, **Figure 6**). This result is also indicative of very limited side reactions involving the furan rings during the high temperature curing process. Temperature screening using 100 mg DGF/MBCA in methanol at 60 to 70 °C for 18 hours (**Figure 3A and 3B**) indicated a 90% recovery of the furan moiety. Upscaling of the DGF/MBCA methanolysis to 5 g allowed for high furan recovery yield of 85% (**Figure 3C**).

Besides MeOH, the depolymerization of DGF/MBCA was investigated using a range of other primary alcohols (ethanol, propanol, butanol). At 60 °C, only MeOH was found capable of efficiently depolymerizing DGF/MBCA (**Figure 3D**). This is attributed to the size and hydrophilic/hydrophobic balance of methanol *vis-à-vis* the overall polarity of the DGF/MBCA

polymer – all contributing to favorable diffusion and dissolution characteristics (*46*). Nonetheless, ethanolysis of DGF/MBCA could be achieved at reaction temperatures of 90 and 120 °C, reaching an ~60% isolated yield of diethyl ester of 2,5-furandicarboxylic acid (DEFD) (**Figure S7-S8**). Furthermore, methanolysis of DGF/MBCA, was also investigated at *room temperature*. After a 3-day long induction period, which we attribute to slow diffusion of the MeOH into the polymeric matrix (*46*), the depolymerization of DGF/MBCA did run to full completion over twenty days (**Figure 3E**).

Comparative depolymerization runs were performed with DGB/MBCA and DGF/DDM. Interestingly, methanolysis of DGB/MBCA was significantly slower compared to DGF/MBCA, indicating the influence of the furan moiety on the depolymerization rate (**Figure 3F**). A clearly beneficial impact of the aliphatic MBCA unit was also seen, since DGF/DDM, comprising an aromatic diamine, remained completely intact.

Importantly, the stability of DGF/MBCA was confirmed in a range of other organic solvents and in acidic/basic aqueous environments after 1 week of storage (**Figure 3G, 3H**). In addition, DMA analysis of DGF/MBCA immersed in water for 72 hours, presented a T_α of 172 °C and a glassy storage modulus of 1.15 GPa (**Figure S46**). These values are practically unchanged compared to the initial DGF/MBCA, demonstrating hydrolysis resistance and stability towards moist environments. All these results underscore the usability of the ERT for a range of relevant application areas, for example in composites, coatings, as well as biomedical devices (*1-3*).

Finally, to demonstrate the broader applicability of the here developed methanolysis protocol, we have synthesized and characterized six additional ERT materials by variation of the dicarboxylic acid and/or amine curing agent (**Supplementary Section 3.18**). These ERTs demonstrated distinct thermal (T_g = 75-180 °C) and mechanical properties (E' = 1.0-2.0 GPa), covering a wide range of properties, depending on the flexibility/rigidity of the used acid/amine backbone. This is beneficial for the potential customization of these ERTs for desired application areas. All new ERT underwent dissolution by methanolysis at 70 °C, albeit to a different extent (20 to 90% dimethyl ester recovered), showing the original DGF/MBCA as the superior material in this library (**Table S10 and Figure S49**).

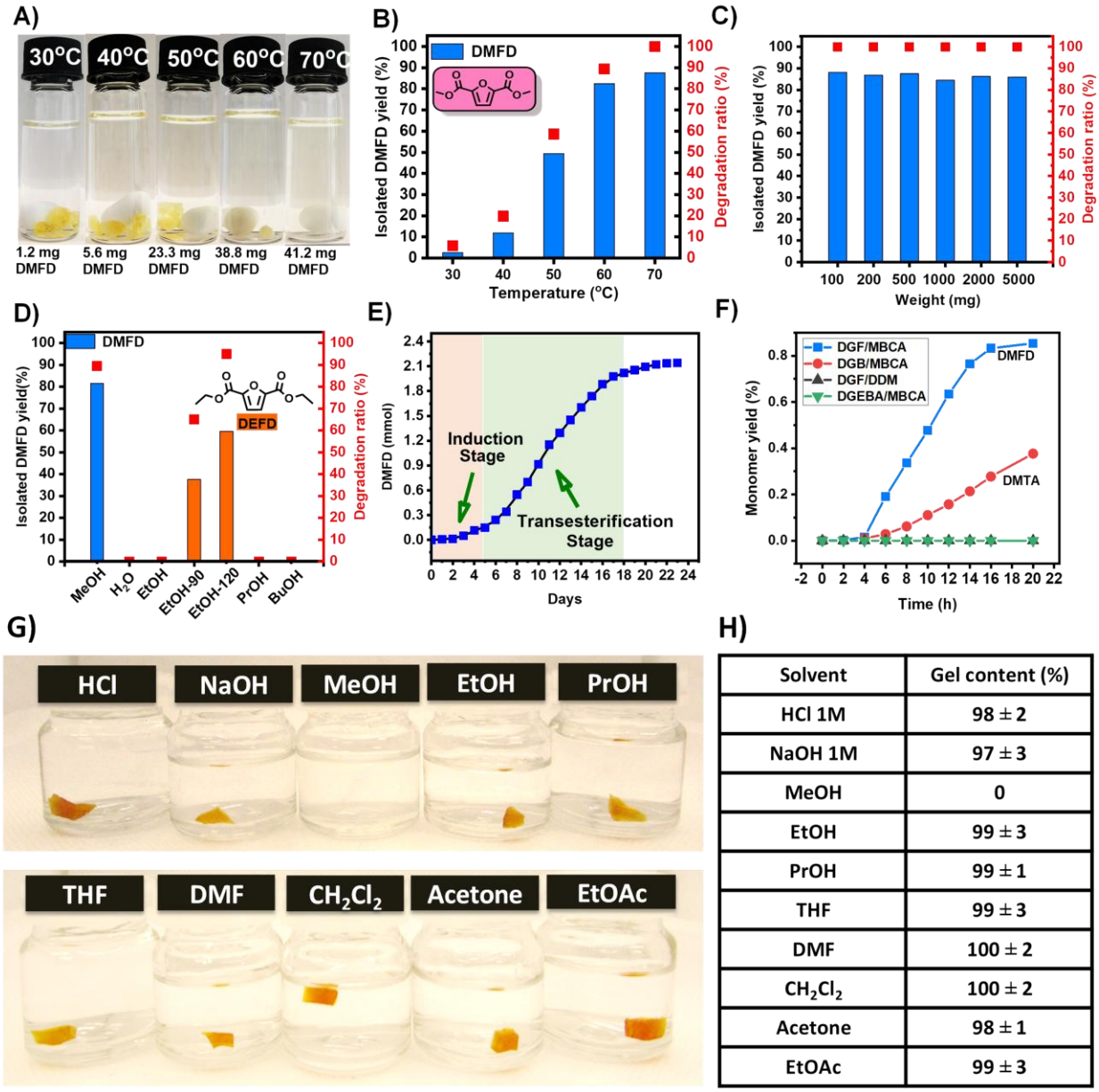

Solvent	Gel content (%)
HCl 1M	98 ± 2
NaOH 1M	97 ± 3
MeOH	0
EtOH	99 ± 3
PrOH	99 ± 1
THF	99 ± 3
DMF	100 ± 2
CH_2Cl_2	100 ± 2
Acetone	98 ± 1
EtOAc	99 ± 3

Figure 3. Investigation of the methanolysis behavior of synthesized epoxy resin materials, and comparative solvent stability. General reaction conditions: 100 mg epoxy resin, 4 mL alcohol, 18 h unless otherwise stated. Isolated yield was obtained by filtration of depolymerized crude products over a short path of silica gel column. A and B) methanolysis of DGF/MBCA at different reaction temperatures for 18 h; C) DGF/MBCA methanolysis at different scales, at 70 °C and for a time period of 24 h (for 100 and 200 mg scale) and 48 h (for 500-5000 mg scale); D) Influence of the solvent on the DGF/MBCA depolymerization, at 60 °C for 18 h; E) Methanolysis time series at room temperature: 1000 mg DGF/MBCA, 100 mL methanol, 200 mg p-xylene as an internal standard; F) Comparative methanolysis of DGF/MBCA, DGB/MBCA and DGF/DDM (400 mg polymer, 50 mL methanol, 70 °C, 100 mg p-xylene as an internal standard); G and H) Chemical stability of DGF/MBCA ERT in different solvents, acidic and basic solutions after one week.

Elucidation of reactivity differences: using model compound studies

The significant methanolysis rate difference between furan-containing DGF/MBCA and its benzene-containing analogue DGB/MBCA as well as the effective non-reactivity of DGF/DDM bearing an aromatic diamine backbone has prompted us to investigate the role of relevant amines in the transesterification reaction. Therefore, we performed a set of small molecule studies, mimicking ester linkages and possible amine environments in cured DGF/MBCA, DGB/MBCA and the non-reactive DGF/DDM. Thus, the methanolysis of simple glycerol esters of furan carboxylic acid (**F1**) and benzoic acid (**B1**) was systematically studied in the presence of aromatic secondary and tertiary amines (**A1** and **A2**, respectively), and their aliphatic amine analogues (**A3** and **A4**) (**Figure 4A, 4B and 4C**). While no transesterification took place in the absence of amine, as expected, both **F1** and **B1** underwent methanolysis in the presence of aliphatic amines (**A3** and **A4**) at 60 °C. More specifically, 90% yield of the corresponding methyl ester was detected applying the furane ester **F1** with both **A3** and **A4**, while **B1** delivered 90% and 40% product yield, using **A3** and **A4**, respectively. The aromatic amines **A1** and **A2** did not show any transesterification activity. Furthermore, ethanolysis of **F1** led to a higher yield of corresponding ethyl ester with **A3**, compared to **B1** (**Table S3** and **S4**). All these observations are perfectly consistent with the results obtained with the cured ERT polymers. Interestingly, hydrolysis of small molecules **F1** and **B1** was facile, unlike the reactivity of the actual ERT materials, which showed high hydrolysis stability due to their hydrophobicity.

To further explain the reactivity difference between DGF/MBCA and DGB/MBCA, kinetic studies were undertaken (**Figure 4D-4H, Supplementary section 3.2**). Plotting the concentration of **F1/B1** versus time revealed zeroth-order rate behavior in the presence of tertiary amine **A3**. Moreover, according to the rate constants measured at different reaction temperatures, the activation energy of transesterification of **F1** was found to be 40.6 kJ/mol, lower than that observed for **B1** (57.2 kJ/mol), being in line with the higher transesterification reactivity of furanic DGF/MBCA over DGB/MBCA. These activation energy values refer to the simple model systems **F1** and **B1,** and not the actual polymers.

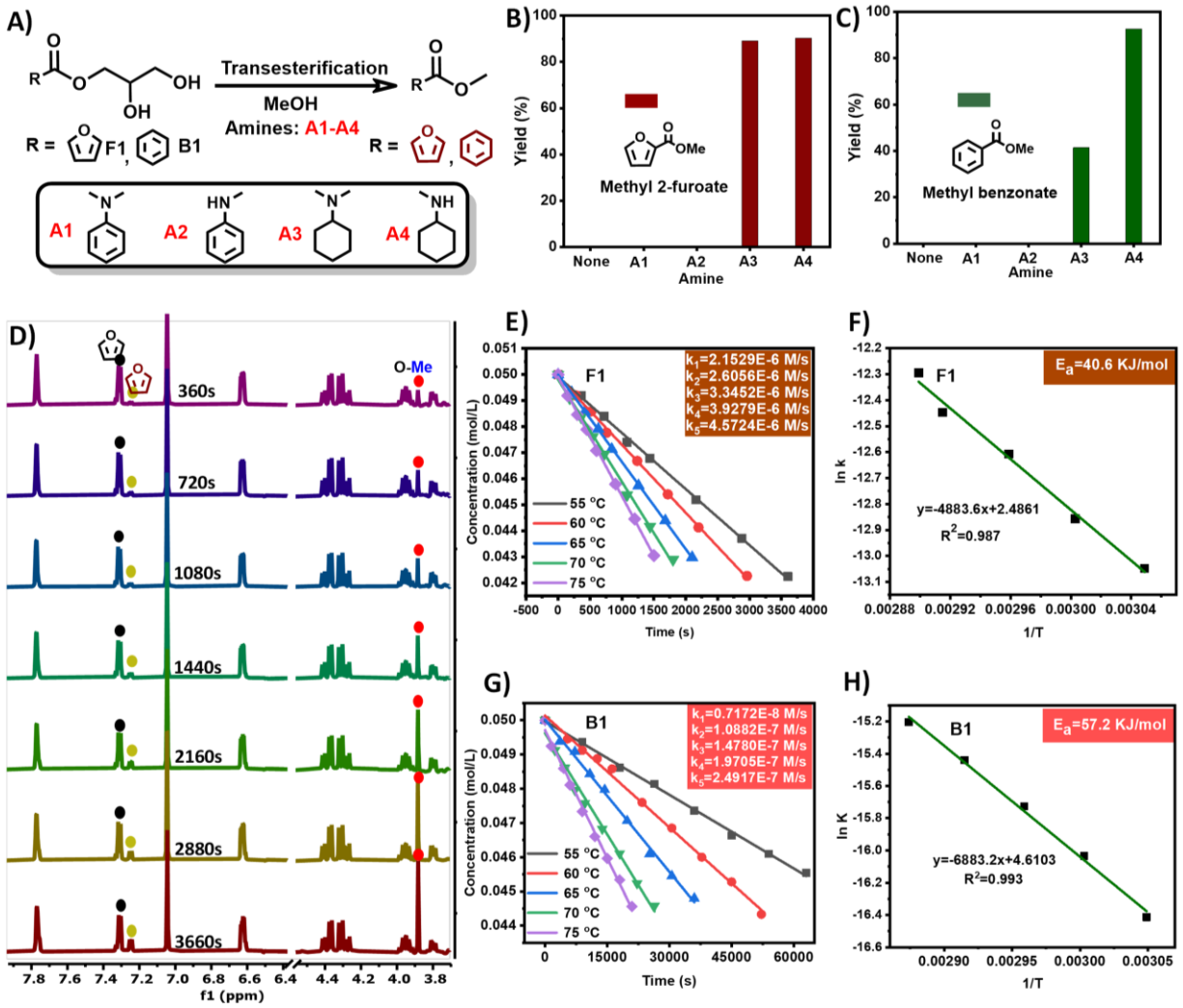

Figure 4. Study of the transesterification reaction of model compounds F1 and B1 catalyzed by amines. A, B, C) Transesterification of **F1** and **B1** in methanol. Reaction conditions: 1 mmol **B1/F1**, 1 equiv. amine, 4 mL methanol, 30 mg p-xylene, 60 °C, 18 h. Yield was determined by ^{1}H NMR spectral integration using p-xylene as internal standard; **D)** ^{1}H-NMR spectral time series of the amine-catalyzed transesterification of model compound **F1. E and G)** Kinetic profiles of the amine-catalyzed transesterification of model compounds **F1/B1** at different reaction temperatures in the presence of **A3**. **F** and **H)** the respective Arrhenius plots (ln k *vs* 1/T) for the data in (**E**) and (**G**). General reaction conditions: 1 mmol substrate, 0.25 mmol amine, 20 mL methanol, 30 mg p-xylene, 55-75 °C; Kinetic data were obtained based on NMR integrated yield using p-xylene as internal standard.

Mechanistic implications

Reflecting upon the obtained results, the ability of the fully cured, typically insoluble thermoset material (DGF/MBCA) to undergo methanolysis at operational temperatures down to room temperature and in the absence of any additive is a remarkable observation. Transesterification of organic esters with methanol, for example in biodiesel production (*48-49*) requires the addition of a strong base (e.g KOH) for methanol deprotonation to generate the nucleophile (*50*). The tertiary amine groups formed in the fully cured ERT backbone play a significant role in the degradation mechanism, however due to their moderate basicity, methanol deprotonation is

thermodynamically highly unfavorable under these conditions (*51*). Considering the pKa of methanol (15.5 at 25 °C) (*52*) versus the pKb of the amine moieties in the formed ERTs (estimated in the range of 6-8 at 25 °C) (*53*), the occurrence of a classical ionic mechanism in our system is highly unlikely (see also **Supplementary Section 3.19**). It is therefore reasonable to propose that ERT methanolysis proceeds by a non-ionic mechanism, and via hydrogen bonding interactions involving the polymer backbone, which promotes its own degradation in methanol. Indeed, previous pioneering work on related ester/amine-based ERT has pointed towards a pronounced hydrogen bonding network in these types of polymers, although their recyclability was not studied (*34*).

Interestingly, H-bonding phenomena are widely observed in organocatalytic and biocatalytic systems (**Figure 5**) (*54-61*). For example, simple amines (alike **A3** and **A4**) in combination with phenol derivatives have been identified as potent organocatalysts in ring opening polymerization of lactides, whereby the reactivity of the primary alcohol is enhanced by H-bonding interaction with the applied tertiary amine (*60*). Furthermore, several important enzyme active sites operate by extensive H-bonding interactions. Exemplary are the 'catalytic triads' comprising specific amino acid motifs (e.g., Ser-His-Asp) in hydrolase enzymes capable of simultaneous carbonyl activation and alcohol deprotonation (*61*).

Thus, we hypothesize that the low temperature methanolysis activity observed in DGF/MBCA is the result of the simultaneous activation of the ester carbonyl group as well as methanol, that way facilitating the required nucleophilic attack, while the proximity of the aliphatic amine moiety (displaying appropriate basicity), is responsible for proton abstraction. The unique arrangement of both MBCA as well as FDCA create the steric/electronic environment necessary for the simultaneous existence of carbonyl and methanol activating hydrogen bonds. This vision is strongly supported by state-of-the-art quantum chemical calculations performed with relevant model compounds, mimicking the more reactive DGF/MBCA, as well as the less reactive DGB/MBCA (**Supplementary Section 3.12**). Calculations were also performed involving larger model structures to capture the nature of DGF/MBCA and DGB/MBCA polymers (**Supplementary Section 3.12F**). These revealed that DGF/MBCA adopts a more open structure compared to DGB/MBCA, whereby DGF/MBCA engages in complex H-bonding interactions, while DGB/MBCA is governed by a variety of benzene-benzene and benzene-cyclohexyl van der Waals interactions. Indeed, methanol has the ability to interfere with the H-bonding network in DGF/MBCA, ultimately occupying favorable depolymerization configurations within the polymer chains.

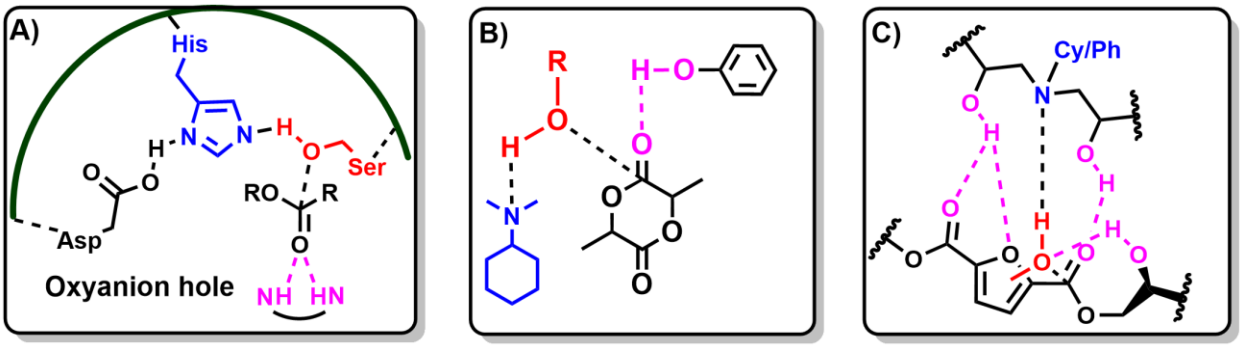

Figure 5. **Non-ionic organocatalytic and biocatalytic transesterification through H-bonding interaction mechanism**. **A**) Schematic description of the amino acid binding motif (Ser-His-Asp) in hydrolase enzymes capable of simultaneous carbonyl activation and alcohol

deprotonation (*61*). **B**) Schematic depiction of H-bonding facilitated polymerization of lactide with primary alcohols (*60*). **C)** Proposed H-bonding facilitated transesterification of DGF/MBCA ERT with methanol supported by quantum chemical calculations (**Supplementary Section 3.12**).

Closed loop recycling of DGF/MBCA ERT

The overall DGF/MBCA depolymerization process, inclusive of the isolated yields of recovered monomers, is depicted in **Figure 6**. Besides the recovery of DMFD, it was also found possible to isolate the polyol residues fraction using a tandem purification protocol consisting of crystallization and fractionation by EtOAc (**Supplementary Section 3.2**). Characterization of post-depolymerization methanol soluble products, originating from DGF/MBCA and DGB/MBCA, by electrospray ionization (ESI) and atmospheric pressure chemical ionization (APCI) qualitatively revealed the respective presence of DMFD and DMTA (**Figure S21**). Importantly, these mixtures did not contain any of the original starting materials, MBCA and the DGF/DGB epoxides. Furthermore, a range of polyol residues bearing secondary and tertiary amines could be identified (**Figure S21, Figure 6 - ^{1}H NMR**) and the occurrence of primary amines in these polyol residues could be excluded. Also, no amides could be observed in the reaction mixtures, an observation which significantly strengthens the hypothesis that the polymerization reaction only involved nucleophilic attack of the amines on epoxy groups.

To achieve closed-loop recycling of the DGF/MBCA thermoset, not only the furan-containing monomer but also the MBCA diamine must be recovered. With the latter recovered as a range of diamine polyols, the challenge of selective dealkylation of the amine groups arose. Gratifyingly, heating said polyol residues in acetic acid at 270 °C allowed for the liberation of acetylated MBCA (**Table S5**) in an encouraging 22% yield. Subsequent hydrolysis of acetylated MBCA easily yields neat MBCA (*62*). Furthermore, it was found that the acetolysis dealkylation process also yields triacetin (**Figure S24**), which is easily reconverted into glycerol (*63*), the starting compound to glycidol (*64*).

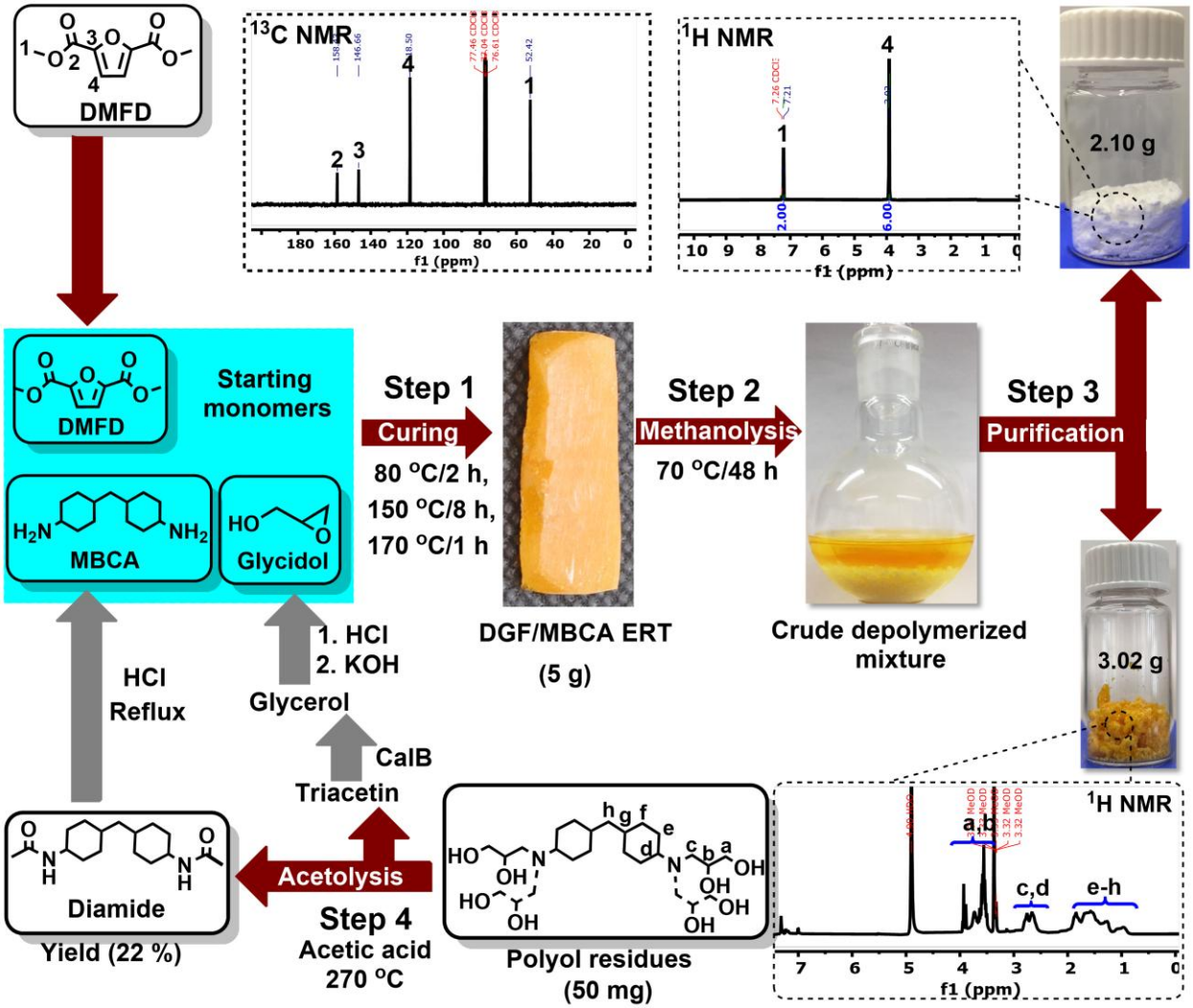

Figure 6. A schematic representation of closed loop recycling of a fully bio-based DGF/MBCA ERT amenable to low-temperature methanolysis. Step 1: Curing conditions: 2 equiv. DGF, 1 equiv. MBCA, 80 °C/2 h, 150 °C for 8 h, 170 °C/1h; **Step 2**: Depolymerization conditions: 5 g DGF/MBCA, 40 mL methanol, 70 °C for 48 h; **Step 3**: Purification protocol involving crystallization and washing with EtOAc, monitored by ^{1}H NMR; **Step 4**: Acetolysis conditions: 50 mg polyol residues, 3 mL acetic acid, 270 °C for 24 h. The red arrows designate methods developed in this work. The gray arrows indicate methods reported in the literature. Details can be found in **Supplementary section 3.13.**

Applications and reuse in fiber composites

Finally, to illustrate the applicability of our DGF/MBCA ERT, glass fiber reinforced composites were synthesized and successfully recycled **(Figure 7A)**. Most interestingly, the acquired SEM images **(Figure 7B)** and FTIR spectra **(Figure 7C)** for pristine and recovered glass fibers are indistinguishable. This result shows that the applied mild methanolysis procedure effectively removes the polymeric matrix but does not affect the glass fiber structure. Encouraged by these results, we set out to apply DGF/MBCA ERT for the development of fully biomass-based plant fiber composites, a particularly interesting research area that is markedly limited by the

availability of suitable biomass-based ERT resins. We here demonstrate proof of principle for the preparation of natural fiber composites, showing good mechanical properties (bending modulus: 17.5 GPa, bending strength: 117.6 MPa) and thermally resistant behavior (T_g =170 °C) using DGF/MBCA **(Figure 7D, Figure S44, S45)**.

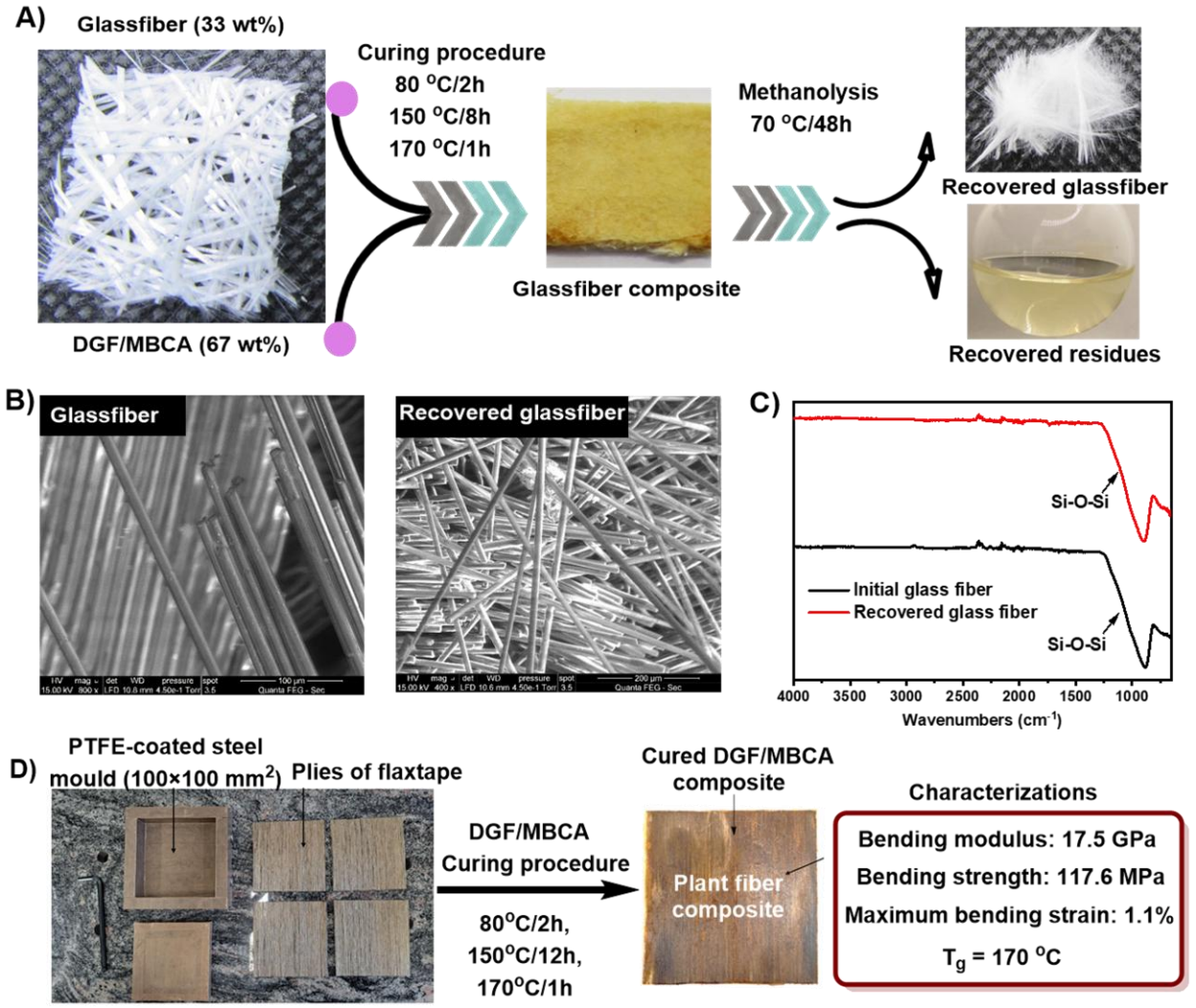

Figure 7. Synthesis and recyclability of DGF/MBCA based glass and wood fiber composites. A) schematic representation of the preparation of DGF/MBCA based glass fiber composites; SEM images (B) and FTIR spectroscopy (C) of DGF/MBCA based glass fiber composites before and after methanolysis. D) Synthesis and characterization of fully bio-based DGF/MBCA wood composites.

Conclusions

The demand for next generation thermosetting materials in critically important industrial segments is gradually increasing, while there is urgent need to adapt circular economy practices to reduce greenhouse gas emissions and overall environmental footprint. Therefore, the development of inherently recyclable and high-performance ERT, derived entirely from renewable resources represents a much-desired research objective. However, thus far this has been challenged by insufficient structural and molecular design. Here we have shown that the judicious combination of building blocks derived from cellulose and lignin leads to a fully bio-

based, performance-privileged ERT, amenable to low temperature methanolysis. The performed kinetic measurements and quantum chemical calculations, including predicted polymer structures, provide strong support for a H-bonding degradation mechanism to be at play, although a simple base-catalyzed scenario cannot be explicitly ruled without further in-depth investigation. This, full material solubilization, followed by our acetolysis step developed - which could potentially be extended to other existing conventional thermoset materials - allows for the recovery of all involved bio-based building blocks. Moreover, due to the favorable thermal and mechanical properties, we were able to prepare reusable glass fiber and plant fiber composites. This, together with the excellent stability of DFG/MBCA in a wide range of organic solvents, and demonstrated inertness toward hydrolysis, underscores the high potential of these furan-ester based ERT in relevant application areas involving sustainable transportation, coatings, paints or biomedical devices. Overall, these findings represent an important step towards the integration of thermosets into the circular and bio-based economy.

Materials and methods

Materials

4,4'-Methylenebis(cyclohexylamine) (mixture of isomers) (>97.0%, TCI), 4,4'-Methylenebis(2-methylcyclohexylamine) (mixture of isomers) (>99.0%, TCI), 1-Amino-3-aminomethyl-3,5,5-trimethylcyclohexane (mixture of isomers) (>99.0%, TCI), Adipic acid (>99.0 %, TCI), 2,5-Furandicarboxylic Acid (>98.0%, TCI), 2-Furancarboxylic Acid (>98%, TCI), Benzoic acid (>99.0%, TCI), Thionyl chloride (≥99.0%, Sigma Aldrich), Triethylamine (≥99.5%, Sigma Aldrich), Glycidol (96%, Sigma Aldrich), Acetic anhydride (≥99.0%, Sigma Aldrich), Terephthalic acid (>99.0%, TCI), 4,4-Diaminodiphenylmethane (>98.0%, TCI), *N*, *N*-dimethylcyclohexylamine (>98.0%, TCI), *N*, *N*-dimethylaniline (>99.0%, TCI), *N*-methylcyclohexylamine (>99.0%, TCI), *N*-methylaniline (>98.0%, TCI), Concentrated H_2SO_4 (95.0-98.0%, Sigma Aldrich), Anhydrous DCM (≥99.8%, Sigma Aldrich), Anhydrous N, N-dimethylformamide (≥99.8%, Sigma Aldrich), Anhydrous Na_2SO_4 (≥99.0%, Sigma Aldrich), Sodium bicarbonate (≥99.7%, Sigma Aldrich), Silica gel for column chromatography (Sigma Aldrich) All chemicals were used as received.

Methods

Synthesis of the DGF/MBCA, DGB/MBCA, DGF/DDM and DGEBA/MBCA ERTs

A range of different epoxy resins were synthesized by using a 2:1 molar ratio of DGF, DGB or DGEBA epoxy monomers and different diamines MBCA or DDM as a curing agent. In a typical procedure, diamine (1 equiv.) and epoxy monomer (2 equiv.) were thoroughly mixed *via* a SpeedMixer for 3 minutes. The mixture was then placed in aluminium mold and cured at 80 °C for 2 h, 150 °C for 8 h and post-cured at 170 °C for 1 h. In the specific case of the DGB epoxy, dichloromethane was added to the initial mixture to assure a proper mixing of this solid epoxy monomer with MBCA before cured. Dichloromethane was then removed under reduced vacuum at 50 °C for 4 h before performing the curing procedure.

Small scaling of methanolysis depolymerization of DGF/MBCA, DGF/DDM, DGB/MBCA and DGEBA/MBCA ERTs

The mild depolymerization of the synthesized DGF/MBCA, DGF/DDM, DGB/MBCA and DGEBA/MBCA ERTs through methanolysis was carried out in a 10 mL pressure tube, equipped with a magnetic stirring bar. Typically, the pressure tube was charged with the respective epoxy resin, such as DGF/MBCA (100 mg), and methanol (4 mL). The pressure tube was sealed and

heated to target temperature while stirring. After completion of the reaction, the methanol was removed under a reduced vacuum, and the resulting mixture was filtered through a thin layer of silica gel using dichloromethane solvent to yield corresponding DMFD or DMTA monomer.

Large scaling of methanolysis depolymerization of DGF/MBCA ERT

The mild depolymerization of the synthesized DGF/MBCA through methanolysis was carried out in a 100 mL single-necked round bottom flask, equipped with a magnetic stirring bar. Typically, the flask was charged with 5 g of DGF/MBCA, and methanol (40 mL). The flask was sealed and heated to 70 °C while stirring for 48 h. After completion of the reaction, the flask was cooled to room temperature and kept for several days until no further crystallization (white solid) was found. Then the crude white solid was filtered and subsequently washed with cold methanol to yield pure DMFD monomer. The residues after filtration were collected and further purified by fractionation with EtOAc several times to get rid of all DMFD monomer (characterized by ^{1}H NMR), providing polyol residues which can be used for further reactions.

Preparation of glass fiber reinforced composite DGF/MBCA ERT

DGF and MBCA monomers were solubilized and diluted in acetone (dichloromethane is also a suitable solvent candidate) (50/50 w/w) and placed in a mold. Glass fiber was then added into this solution and allowed to soak for 2 h, offering ample time for the epoxy resin to impregnate glass fiber network. The acetone was subsequently completely removed under reduced vacuum at 30 °C for 4 h. Following this, the mixture was cured at 80 °C for 2 h and at 150 °C for 8 h. Additionally, a post-curing treatment was also performed at 170 °C for 1 h.

Preparation of wood fiber reinforced composite DGF/MBCA ERT

In a typical procedure, DGF and MBCA monomers (71.8/28.2 w/w) were thoroughly mixed and solubilized in acetone (50/50 w/w) and poured into the mold stacked with flax plies with an aerial weight of 110 g/m². Then the mold was closed and dried under a reduced vacuum at ambient temperature for 3 h before undergoing a hot press for curing. When a temperature of 80 °C was reached in the mold, a pressure of 4 bars was applied and maintained for 2 h at 80 °C and then for 12 h at 150 °C. After completion of the curing process, the mold was cooled to room temperature and was removed from the hot press. Finally, the unmolded wood fiber composite was subjected to a post-curing process at 170 °C in an oven for 1 h.

Kinetic studies with model compounds

Transesterification of the synthesized glycerol ester of 2-furancarboxylic acid (**F1**) and glycerol ester of benzoic acid (**B1**) using methanol in the presence of *N*, *N*-dimethylcyclohexylamine was carried out in a 100 mL single-necked round bottom flask, equipped with a magnetic stirring bar. Typically, the flask was charged with 186 mg, 1 mmol **F1** or 1 mmol, 196 mg **B1**, methanol (20 mL), 0.25 equiv. *N*, *N*-dimethylcyclohexylamine at 55-75 °C and 30 mg p-xylene. Then, the flask was sealed and heated to target temperature while stirring. Each sample (~ 0.2 mL) taken from the flask at different reaction time was diluted by MeOH-d4 (0.3 mL) and was subsequently subjected to quantitative ^{1}H NMR analysis. The initial rate is calculated at a conversion below 20%.

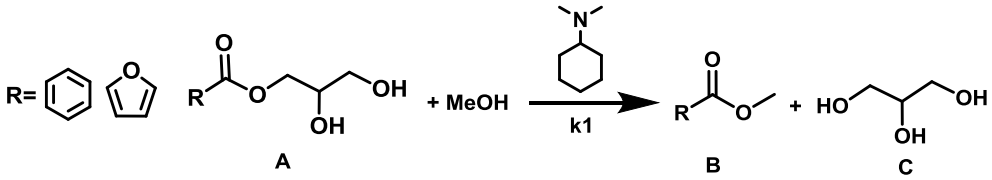

A B C

A pseudo-homogeneous kinetics model has been used to describe the conversion of A into B to determine rate laws and kinetic parameters based on the experimental data obtained. The reaction is dependent upon the concentration of A and MeOH. Since MeOH was present in large excess, the concentration of MeOH was considered as constant as the reaction proceeds. For the above-mentioned reaction, the rate equation can be given as,

$$Rate = -\frac{d[CA]}{dt} = k1[CA]^{\alpha}[MeOH]^{\beta} \qquad eq1$$

$$Rate = -\frac{d[CA]}{dt} = k1[CA]^{\alpha} \qquad eq2$$

The rate constant *k1* and reaction order α at different reaction temperatures (55 °C, 60 °C, 65 °C, 70 °C and 75 °C) were determined by plotting [CA] as a function of time. Based on the experimental data obtained, the concentration of [CA] decreases linearly as a function of time, which means that the reaction rate is independent of concentration of [CA]. In other words, the order α of transesterification of A in methanol with respect to A is 0. Thus the rate law can be given as:

$$Rate = -\frac{d[CA]}{dt} = k1 \qquad eq3$$

$$[CA] = k1t + C \qquad eq4$$

Based the rate constant k obtained above at different reaction temperature, we thus can further calculate the activation energy for transesterification of A, following the Arrhenius equation below:

$$Ink = -\frac{Ea}{RT} + In\,A \qquad eq5$$

The experimental activation energy (Ea) at different reaction temperatures (55 °C, 60 °C, 65 °C, 70 °C and 75 °C) can be determined by plotting Ink as a function of -1/T where the slope is -Ea/R

DFT calculations for mechanistic elucidation

All DFT calculations were done with TURBOMOLE 7.5.1. Geometries were optimized employing the PBE functional together with the D3 dispersion correction using Becke-Johnson damping and the def2-SVPD basis set. For speeding up the calculations, the resolution of identity (RI) approximation was utilized. NBO-charges were calculated with the NBO implementation of TURBOMOLE at the B3LYP-D3BJ/def2-TZVPPD@PBE-D3BJ/def2-SVPD level while making use of the RIJK approximation. All DFTB calculations were performed with DFTB+ 22.1 *via* the use of the respective interface of the atomic simulation environment (ASE). Self-consistent-charge Third Order Density Functional Tight Binding (DFTB3) was used throughout, employing the 3ob-3-1 parameter set, the D3 dispersion correction using Becke-Johnson damping and the D3H5 correction for the description of hydrogen bonds, as in other cases the interaction between

hydroxyl groups and amine moieties was found to be underrepresented when compared to DFT optimizations on small model structures. The convergence criterium for the charges was set to 10^{-9}. Geometry optimizations were carried out with the BFGS implementation of ASE, employing a convergence criterium of 0.001 eV/Å. Pictures of the 3D-geometries were generated with JMOL and VMD (more details can be found in **Supplementary section 3.12**).

References and Notes

1. F. L. Jin, X. Li, S. J. Park, Synthesis and application of epoxy resins: A review. *J. Ind. Eng. Chem.* **29**, 1-11 (2015).
2. J.-P. Pascault, R. Williams, in Thermosets. *Elsevier*, 3-34 (2018).
3. May, C. A., Epoxy Resins, Chemistry and Technology, Routledge 2018.
4. M. MacLeod, H. P. H. Arp, M. B. Tekman, A. Jahnke, The global threat from plastic pollution. *Science* **373**, 61-65 (2021).
5. https://www.epa.gov/regulatory-information-topic/regulatory-and-guidance-information-topic-waste
6. https://www.epa.gov/sites/default/files/2015-09/documents/bpa_action_plan.pdf
7. B. S. Rubin, Bisphenol A: An endocrine disruptor with widespread exposure and multiple effects. *J. Steroid. Biochem.* **127**, 27-34 (2011).
8. J. S. Mahajan, R. M. O'Dea, J. B. Norris, L. T. Korley, T. H. Epps III, Aromatics from lignocellulosic biomass: a platform for high-performance thermosets. *ACS Sustainable Chem. Eng.* **8**, 15072-15096 (2020).
9. R. M. Cywar, N. A. Rorrer, C. B. Hoyt, G. T. Beckham, E. Y.-X. Chen, Bio-based polymers with performance-advantaged properties. *Nat. Rev. Mater.* **7**, 83-103 (2022).
10. J.-G. Rosenboom, R. Langer, G. Traverso, Bioplastics for a circular economy. *Nat. Rev. Mater.* **7**, 117-137 (2022).
11. R. Auvergne, S. Caillol, G. David, B. Boutevin, J.-P. Pascault, Biobased thermosetting epoxy: present and future. *Chem. Rev.* **114**, 1082-1115 (2014).
12. T. E. Long, Toward recyclable thermosets. *Science* **344**, 706-707 (2014).
13. N. Zheng, Y. Xu, Q. Zhao, T. Xie, Dynamic covalent polymer networks: a molecular platform for designing functions beyond chemical recycling and self-healing. *Chem. Rev.* **121**, 1716-1745 (2021).
14. Y. Jin, Z. Lei, P. Taynton, S. Huang, W. Zhang, Malleable and recyclable thermosets: The next generation of plastics. *Matter* **1**, 1456-1493 (2019).
15. F. García, M. M. Smulders, Dynamic covalent polymers. *J. Polym. Sci. Polym. Chem.* **54**, 3551-3577 (2016).
16. D. J. Fortman *et al.*, Approaches to sustainable and continually recyclable cross-linked polymers. *ACS Sustainable Chem. Eng.* **6**, 11145-11159 (2018).
17. P. Shieh, J. A. Johnson *et al.* Cleavable comonomers enable degradable, recyclable thermoset plastics. *Nature* **583**, 542–547 (2020).

18. S. Zhao, M. M. Abu-Omar, Recyclable and malleable epoxy thermoset bearing aromatic imine bonds. *Macromolecules* **51**, 9816-9824 (2018).
19. B. Wang *et al.*, Facile synthesis of "digestible", rigid-and-flexible, bio-based building block for high-performance degradable thermosetting plastics. *Green Chem.* **22**, 1275-1290 (2020).
20. L. Zhong *et al.*, Closed-loop recyclable fully bio-based epoxy vitrimers from ferulic acid-derived hyperbranched epoxy resin. *Macromolecules* **55**, 595-607 (2022).
21. X. Chen *et al.*, Degradable and recyclable bio-based thermoset epoxy resins. *Green Chem.* **22**, 4187-4198 (2020).
22. R. Dinu, A. Pidvoronia, U. Lafont, O. Damiano, A. Mija, High performance, recyclable and sustainable by design natural polyphenol-based epoxy polyester thermosets. *Green Chem.* **25**, 2327-2337 (2023).
23. W. Zhang *et al.*, Recyclable, Degradable, and Fully Bio-Based Covalent Adaptable Polymer Networks Enabled by a Dynamic Diacetal Motif. *ACS Sustainable Chem. Eng.* **11**, 3065-3073 (2023).
24. Y. Liu *et al.*, Closed-loop chemical recycling of thermosetting polymers and their applications: A review. *Green Chem.* **24**, 5691-5708 (2022).
25. P. R. Christensen, A. M. Scheuermann, K. E. Loeffler, B. A. Helms, Closed-loop recycling of plastics enabled by dynamic covalent diketoenamine bonds. *Nat. Chem.* **11**, 442-448 (2019)
26. Z. Lei *et al.*, Recyclable and malleable thermosets enabled by activating dormant dynamic linkages. *Nat. Chem.* **14**, 1399-1404 (2022).
27. A. Ahrens *et al.*, Catalytic disconnection of C–O bonds in epoxy resins and composites. *Nature* **617**, 730-737 (2023).
28. J. Li *et al.*, A promising strategy for chemical recycling of carbon fiber/thermoset composites: self-accelerating decomposition in a mild oxidative system. *Green Chem.* **14**, 3260-3263 (2012).
29. T. Deng *et al.*, Cleavage of C–N bonds in carbon fiber/epoxy resin composites. *Green Chem.* **17**, 2141-2145 (2015).
30. C. A. Navarro *et al.*, Catalytic, aerobic depolymerization of epoxy thermoset composites. *Green Chem.* **23**, 6356-6360 (2021).
31. J. Deng, X. Liu, C. Li, Y. Jiang, J. Zhu, Synthesis and properties of a bio-based epoxy resin from 2, 5-furandicarboxylic acid (FDCA). *RSC Adv.* **5**, 15930-15939 (2015).
32. J. Meng *et al.*, New ultrastiff bio-furan epoxy networks with high Tg: Facile synthesis to excellent properties. *Eur. Polym. J.* **121**, 109292 (2019).
33. T. P. Kainulainen, P. Erkkilä, T. I. Hukka, J. A. Sirviö, J. P. Heiskanen, Application of furan-based dicarboxylic acids in bio-derived dimethacrylate resins. *ACS Appl. Polym. Mater.* **2**, 3215-3225 (2020).
34. Y. Liu *et al.*, Comparative study on the properties of epoxy derived from aromatic and heteroaromatic compounds: the role of hydrogen bonding. *Ind. Eng. Chem. Res.* **59**, 1914-1924 (2020).

35. E. Manarin, F. Da Via, B. Rigatelli, S. Turri, G. Griffini, Bio-Based Vitrimers from 2, 5-Furandicarboxylic Acid as Repairable, Reusable, and Recyclable Epoxy Systems. *ACS Appl. Polym. Mater.* **5**, 828-838 (2023).

36. N. Eid, B. Ameduri, B. Boutevin, Synthesis and properties of furan derivatives for epoxy resins. *ACS Sustainable Chem. Eng.* **9**, 8018-8031 (2021).

37. J.-T. Miao, L. Yuan, Q. Guan, G. Liang, A. Gu, Biobased heat resistant epoxy resin with extremely high biomass content from 2, 5-furandicarboxylic acid and eugenol. *ACS Sustainable Chem. Eng.* **5**, 7003-7011 (2017).

38. E. d. de Jong, M. Dam, L. Sipos, G.-J. Gruter, in Biobased monomers, polymers, and materials. *ACS Publications*, 1-13 (2012).

39. https://www.avantium.com/wp-content/uploads/2021/04/20210407-Avantium-reaches-key-commercial-milestone-for-its-FDCA-flagship-plant-with-commitments-for-over-50-of-its-output.pdf

40. A. Marotta, V. Ambrogi, P. Cerruti, A. Mija, Green approaches in the synthesis of furan-based diepoxy monomers. *RSC Adv.* **8**, 16330-16335 (2018).

41. X. Wu, M. V. Galkin, K. Barta, A well-defined diamine from lignin depolymerization mixtures for constructing bio-based polybenzoxazines. *Chem Catal.* **1**, 1466-1479 (2021).

42. https://www.spacematdb.com/spacemat/manudatasheets/Epon828.pdf

43. S. You, S. Ma, J. Dai, Z. Jia, X. Liu and J. Zhu, Hexahydro-*s*-triazine: A Trial for Acid-Degradable Epoxy Resins with High Performance, *ACS Sustainable Chem. Eng*. **5**, 4683-4689 (2017).

44. W. Yuan et al., Synthesis of fully bio-based diepoxy monomer with dicyclo diacetal for high-performance, readily degradable thermosets. *Eur. Polym. J.* **117**, 200-207 (2019).

45. M. Janvier, L. Hollande, A. S. Jaufurally, M. Pernes, R. Ménard, M. Grimaldi, J. Beaugrand, P. Balaguer, P.-H. Ducrot, F. Allais, Syringaresinol: A Renewable and Safer Alternative to Bisphenol A for Epoxy-Amine Resins. *ChemSusChem* **10**, 738–746 (2017).

46. X. Kuang *et al.*, Dissolution of epoxy thermosets via mild alcoholysis: the mechanism and kinetics study. *RSC Adv.* **8**, 1493-1502 (2018).

47. X. Zhao *et al.*, Multicycling of Epoxy Thermoset Through a Two- Step Strategy of Alcoholysis and Hydrolysis using a Self- Separating Catalysis System. *ChemSusChem* **15**, e202101607 (2022).

48. H. Fukuda, A. Kondo, H. Noda, Biodiesel fuel production by transesterification of oils. *J. Biosci. bioeng.* **92**, 405-416 (2001).

49. L. Meher, D. V. Sagar, S. Naik, Technical aspects of biodiesel production by transesterification—a review. *Renew. Sust. Energ. Rev.* **10**, 248-268 (2006).

50. J. Otera, Transesterification. *Chem. Rev.* **93**, 1449-1470 (1993).

51. R. B. Grossman, The Art of Writing Reasonable Organic Reaction Mechanisms-Third Edition, *Springer*, 2019. https://doi.org/10.1007/978-3-030-28733-7.

52. D. Gao, Acidities of water and methanol in aqueous solution and DMSO. *J. Chem. Educ.* **86**, 864-868 (2009).

53. https://www.chembk.com/en/chem/Triethanolamine

54. J. J. Garrido-Gonzalez *et al.*, An enzyme model which mimics chymotrypsin and N-terminal hydrolases. *ACS Catal.* **10**, 11162-11170 (2020).

55. J. J. Garrido- González et al., Transesterification of Non- Activated Esters Promoted by Small Molecules Mimicking the Active Site of Hydrolases. *Angew. Chem. Int. Edit*. **61**, e202206072 (2022).

56. A. P. Dove, R. C. Pratt, B. G. Lohmeijer, R. M. Waymouth, J. L. Hedrick, Thiourea-based bifunctional organocatalysis: Supramolecular recognition for living polymerization. *J. Am. Chem. Soc.* **127**, 13798-13799 (2005).

57. A. Chuma *et al.*, The reaction mechanism for the organocatalytic ring-opening polymerization of l-lactide using a guanidine-based catalyst: hydrogen-bonded or covalently bound? *J. Am. Chem. Soc.* **130**, 6749-6754 (2008).

58. M. Reetz, B. List, S. Jaroch, H. Weinmann, *Organocatalysis*. (Springer Science & Business Media, 2008).

59. B. Lin, R. M. Waymouth, Urea anions: simple, fast, and selective catalysts for ring-opening polymerizations. *J. Am. Chem. Soc.* **139**, 1645-1652 (2017).

60. C. Thomas *et al.*, Phenols and Tertiary Amines: An Amazingly Simple Hydrogen- Bonding Organocatalytic System Promoting Ring Opening Polymerization. *Adv. Syn. Catal.* **353**, 1049-1054 (2011).

61. J. J. Garrido-Gonzalez *et al.*, An enzyme model which mimics chymotrypsin and N-terminal hydrolases. *ACS Catal.* **10**, 11162-11170 (2020).

62. Gribble, G. W., Mosher, M. D., Jaycox, G. D., Cory, M., Fairley, T. A., Potential DNA *Bis*-Intercalating Agents. Synthesis and Antitumor Activity of *N,N*-(Methylenedi-4,1-cyclohexanediyl-*bis*(9-acridinamine) Isomers, *Heterocycles*, 88, 535-546 (2014).

63. A. J. Kotlewska, F. van Rantwijk, R. A. Sheldon, I. W. Arends, Epoxidation and Baeyer–Villiger oxidation using hydrogen peroxide and a lipase dissolved in ionic liquids. *Green Chem.* **13**, 2154-2160 (2011).

64. D. Cespi *et al.*, A simplified early-stage assessment of process intensification: glycidol as a value-added product from epichlorohydrin industry wastes. *Green Chem.* **18**, 4559-4570 (2016).

ACKNOWLEDGMENTS

The authors thank Prof. Yuriy Roman of MIT for valuable support and discussion.

Funding:

K. B. is grateful for financial support from the European Research Council, ERC Starting Grant 2015 (CatASus) 638076. X.W. is grateful for financial support from the China Scholarship Council (grant number 201808330391).

Author contributions:

Conceptualization: XYW, KB

Data collection: XYW, PH, DB, FC, VP

Formal Analysis: XYW, PH, DB, MDB, FC, JMZ, ZW, VP

Funding Acquisition: KB

Investigation: XYW, PH, DB, MDB, FC, JMZ, VP, ADB, SC, KB

Methodology: XYW, PH, DB, MDB, VP, ADB, SC, KB

Project administration: KB

Supervision: KB, ADB, VP

Visualization: XYW, PH

Writing – original draft: XYW, KB

Writing – review & editing: XYW, PH, MDB, VP, ADB, SC, KB

Competing interests: XYW, MDB and KB have filed a priority patent application.

Data and materials availability: All data are available in the main text or the supplementary materials.

SUPPLEMENTARY MATERIALS

Supplementary Text

Figures S1 to S51

Tables S1 to S10

References (*65-123*)